

**AN ORDER-OF-MAGNITUDE ESTIMATE OF OCEAN THERMAL ENERGY
CONVERSION (OTEC) RESOURCES**

G rard C. NIHOUS

Associate Researcher

Hawaii Natural Energy Institute, University of Hawaii, Honolulu, HI 96822, U.S.A.

Abstract

Worldwide power resources that could be extracted from the steady-state operation of Ocean Thermal Energy Conversion (OTEC) plants are estimated using a simple model. This order-of-magnitude analysis indicates that about 3×10^9 kW (3 TW) may be available at most. This value is much smaller than estimates currently suggested in the technical literature. It reflects the scale of the perturbation caused by massive OTEC seawater flow rates on the thermal structure of the ocean. Not surprisingly, maximum OTEC power nearly corresponds to deep cold seawater flow rates of the order of the average abyssal upwelling representative of the global thermohaline circulation.

1.0 INTRODUCTION

Ocean Thermal Energy Conversion (OTEC) is an old concept that aims to tap solar energy stored as sensible heat in the upper mixed layer of tropical oceans [1, 2]. Deep cold seawater originally formed at polar margins provides the low temperature needed for an

appropriate working fluid (such as ammonia) to complete a thermodynamic (e.g. Rankine) cycle; the mechanical work produced is easily convertible to electricity. Because practical temperature differences are only of the order of 20°C, with much of this resource needed in the process heat exchangers, the cycle thermodynamic efficiency is of the order of 3%. As a result, several cubic meters per second of seawater are necessary to produce just one megawatt of net electricity. Such facts have so far prevented OTEC and some of its byproducts from being economically competitive. More details can be found in a number of informative synoptic summaries [3-8].

In spite of the challenges faced by OTEC pioneers and enthusiasts in the past several decades, future energy markets may sufficiently change that the vast baseload OTEC resource may become attractive, at least in some special niches. An interesting theoretical question is how large a resource OTEC really is. Not too much emphasis is given to this perhaps academic issue in basic OTEC texts. Meanwhile, worldwide demand for power in general and electricity in particular has rapidly grown. An analysis of the global energy market was recently published by the U.S. Department of Energy (*International Energy Outlook 2004*) [9]. Historical data through 2001 and mid-term projections from 2010 are displayed in Fig. 1 for marketed primary energy¹ (fossil fuels, as well as electricity from nuclear and renewable sources.) A seemingly inexhaustible reserve 50 years ago may be quite insufficient today.

¹Worldwide electrical power consumption, which represents for the most part secondary energy from power plants using fossil fuels, is projected to grow from 1.5 TW in 2001 to 2.7 TW in 2025. Installed capacity for electricity production was 3.5 TW in 2002 (<http://www.eia.doe.gov/aer/txt/ptb1117.html>).

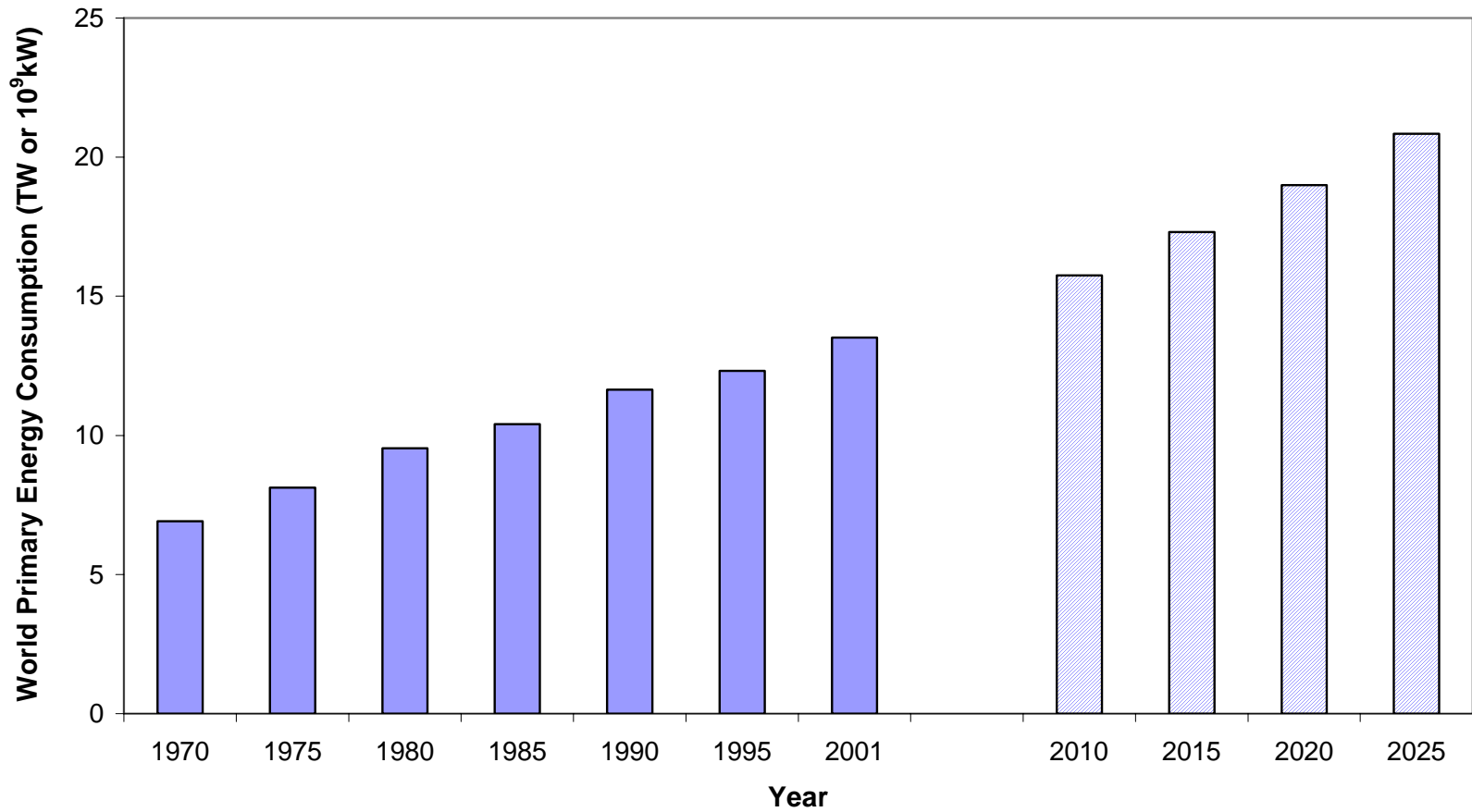


Figure 1 - Recent and projected World power demand (http://www.eia.doe.gov/oiaf/ieo/excel/figure_2data.xls)

Zener [10, 11] recognized in the seventies that ‘Society will not allow any large-scale activity without a prior examination of potential environmental effects.’ He did not explicitly predict a limit for OTEC power, but concluded that a production of 60 TW would not have adverse impacts (e.g. a 1°C cooling of the tropical ocean surface with compensating effects.)

OTEC texts and articles usually refer to incident solar power absorbed in the oceans as a sufficient yardstick to size the OTEC resource. It is often expressed in ‘barrels of oil equivalent’ (boe) over the warmest oceans, e.g. 250 billion boe per day over 60 million km² [7, 12.] This figure can easily be translated into some electrical production potential, as in Table 1.

Noting that the average incident solar power absorbed by the world’s oceans is about 240 W/m², Vega [6] chooses instead the smaller flux corresponding to evaporation as a reference, i.e. 95 W/m². This flux is an example of the natural conversion of solar energy (into latent heat.) Vega [6] proceeds to scale the OTEC resource by using a 3% cycle efficiency on the evaporative flux over the 370 million km² covered by the world’s oceans. This implicitly yields a resource estimate of about 1000 TW (10¹² kW). He then notes that 1% of this amount is of the same order of magnitude as the current worldwide power demand.

After the usual reference to solar power absorbed by the oceans, Johnson [4] notes that the sustainability of the OTEC resource must be limited by the rate of formation of the deep cold seawater. He then quotes an OTEC resource of 50 to 150 TW, but without details.

In the first page of their text, Avery and Wu [5] recognize that there is an upper bound for continuous OTEC operation beyond which significant environmental effects would be incurred; they give a limit of 190 kW of net OTEC power per km² without details; over 100 million km² (10¹⁴ m²) of tropical oceans, this would indicate an OTEC resource of 19 TW.

Table 1 - Summary of OTEC power limits from the technical literature

| <u>Source</u> | <u>OTEC power limit (TW)</u> |
|---|---------------------------------------|
| Incident solar power over 60 million km ² (tropical oceans): 250 billions barrels of oil equivalent (boe) daily [7, 12] | 366 ^{ab} -610 ^{abc} |
| Evaporative flux over all oceans (370 million km ²) and 3% OTEC conversion efficiency [6] | 180 ^{bc} -1000 |
| Limited by the rate of formation of deep water (no details) [4] | 50-150 |
| Environmentally safe OTEC production density: 190 kW/km ² (no details) [5] | 19 ^c |
| Continuous, renewable OTEC production with no detrimental effect on the oceanic thermal structure (no details) [3, 8] | 10 |
| Projected OTEC production of 60 TW deemed safe [10, 11] | > 60 |
| Projected OTEC production of 0.2 TW over 1 million km ² not sustainable [13] | < 20 |

^a 1 boe is 6 million BTU, or 6.326×10^{-3} TJ

^b a net OTEC conversion efficiency of 2% was applied (Standard OTEC Process described in Section 2.0)

^c an area of 100 million km² was used

Finally, Penney and Daniel [3] and Daniel [8] cap the OTEC resource at 10 TW, but once more, the ‘calculations’ or ‘various methods’ that lead to this estimate are omitted. They associate the limit with ‘a continuous, renewable basis’, whereby electricity ‘could be extracted without significantly changing the thermal structure of the ocean.’ The mention of an OTEC heat load of 7 billion boe per day associated with the 10 TW electrical output [3] suggests a net OTEC conversion efficiency of the order of 2%. As discussed in Section 2, this represents a standard value for the OTEC process with typical seawater temperatures; it confirms the authors’ assessment that the thermal structure of the ocean would not substantially be perturbed.

Martin and Roberts [13] published an elegant time-domain model of the operation of 1000 200 MW OTEC plants in the Gulf of Mexico (about 10^{12} m².) They showed that such a scenario was not sustainable, as the available OTEC temperature difference would keep decreasing over time; crudely extrapolated over the tropical oceans (about 10^{14} m²), even though the relatively closed Gulf of Mexico may behave quite differently from large open oceanic areas, this OTEC production would correspond to worldwide resources of 20 TW.

Table 1 summarizes explicit or implicit OTEC resource limits found in (or inferred from) the technical literature. Estimates based solely on solar power absorbed by the ocean or some derivative flux appear much too large (several hundreds TW.) When further limitations inherent to the OTEC process are considered, a wide range of 10 to 150 TW is quoted without details.

The following study is an elementary attempt to realistically provide an order-of-magnitude estimate of OTEC resources. Section 2.0 describes a standard OTEC process and a one-dimensional steady-state model of the vertical structure of oceanic temperature. Section 3.0 provides results from these algorithms in the form of steady-state OTEC resource limits.

2.0 MODEL DESCRIPTION

2.1 Standard OTEC Process

A standard OTEC process is adopted here with little loss of generality, even though operational adaptability may help optimizing the utilization of limited and changing OTEC resources. Calling ΔT the available OTEC temperature difference between surface and deep ocean waters, it typically is broken down into a ‘temperature ladder.’ From a simple optimization procedure [4], it can be shown that the temperature drop across the power-generating turbine is about $\Delta T/2$. The maximum thermodynamic efficiency of an ideal Rankine OTEC power cycle then is very closely approximated by $\Delta T/(2T)$, where T is the surface water temperature. Irreversibilities in the working-fluid expansion (turbine) and compression (pump) occur in real machines. These departures from an ideal Rankine cycle, as well as small losses in the electrical conversion step (generator) are taken into account with a 15% reduction in gross electrical power output (turbogenerator efficiency ε_{tg} of 85%.) With representative values $\Delta T = 20^\circ\text{C}$ and $T = 25^\circ\text{C}$ (298.15 K in the formula), the gross OTEC conversion efficiency is $\alpha \approx \varepsilon_{tg}\Delta T/(2T) = 2.85\%$. In other words, OTEC is a rather inefficient process, though the resource is abundant and renewable.

The case is considered where twice as much warm surface water Q_{ww} as cold deep water Q_{cw} is used, i.e. $Q_{cw} = \eta Q_{ww}$ with $\eta = 0.5$. This typical choice [14, 15] reflects the more immediate availability of surface water; in specific designs, η would be optimized. To determine the rest of the OTEC ‘temperature ladder,’ a minimum approach (pinch) temperature of $\Delta T/16$ (1.25°C at standard conditions) in either evaporator or condenser is

chosen to maintain the exchange of heat. Since the energy extracted in the OTEC process is small relatively to the heat-exchanger loads, it can be neglected in a simplified heat-and-mass balance. It follows that the surface seawater cools by $\{3\eta/(1 + \eta)\} \Delta T/8$ in the evaporator, and the deep seawater warms by $\{3/(1 + \eta)\} \Delta T/8$ in the condenser. The ‘temperature ladder’ as well as a basic OTEC energy budget are illustrated in Figure 2.

The gross electrical power P_g generated is written as the product of the evaporator heat load and the gross OTEC conversion efficiency:

$$P_g = \frac{Q_{ww} \rho c_p 3\eta \varepsilon_{tg}}{16(1 + \eta)T} \Delta T^2 \quad (1)$$

where ρ is an average seawater density, say 1025 kg/m^3 , and c_p is the specific heat of seawater, about 4 kJ/kg-K .

It can be seen from Eq. (1) that a 1°C loss in the resource ΔT , with a baseline value of 20°C , results in a 10% decrease in P_g . This highlights the sensitivity of OTEC operations to ΔT . Finally, the net power P_{net} must be estimated, since it takes a considerable power consumption to drive the large seawater flow rates through an OTEC plant. Most designs typically require about 30% of P_g to run the plant at design conditions [14, 15]. It follows that P_{net} approximately may be written:

$$P_{net} = \frac{Q_{ww} \rho c_p 3\eta \varepsilon_{tg}}{16(1 + \eta)T} \{ \Delta T^2 - 0.3 \Delta T_{design}^2 \} \quad (2)$$

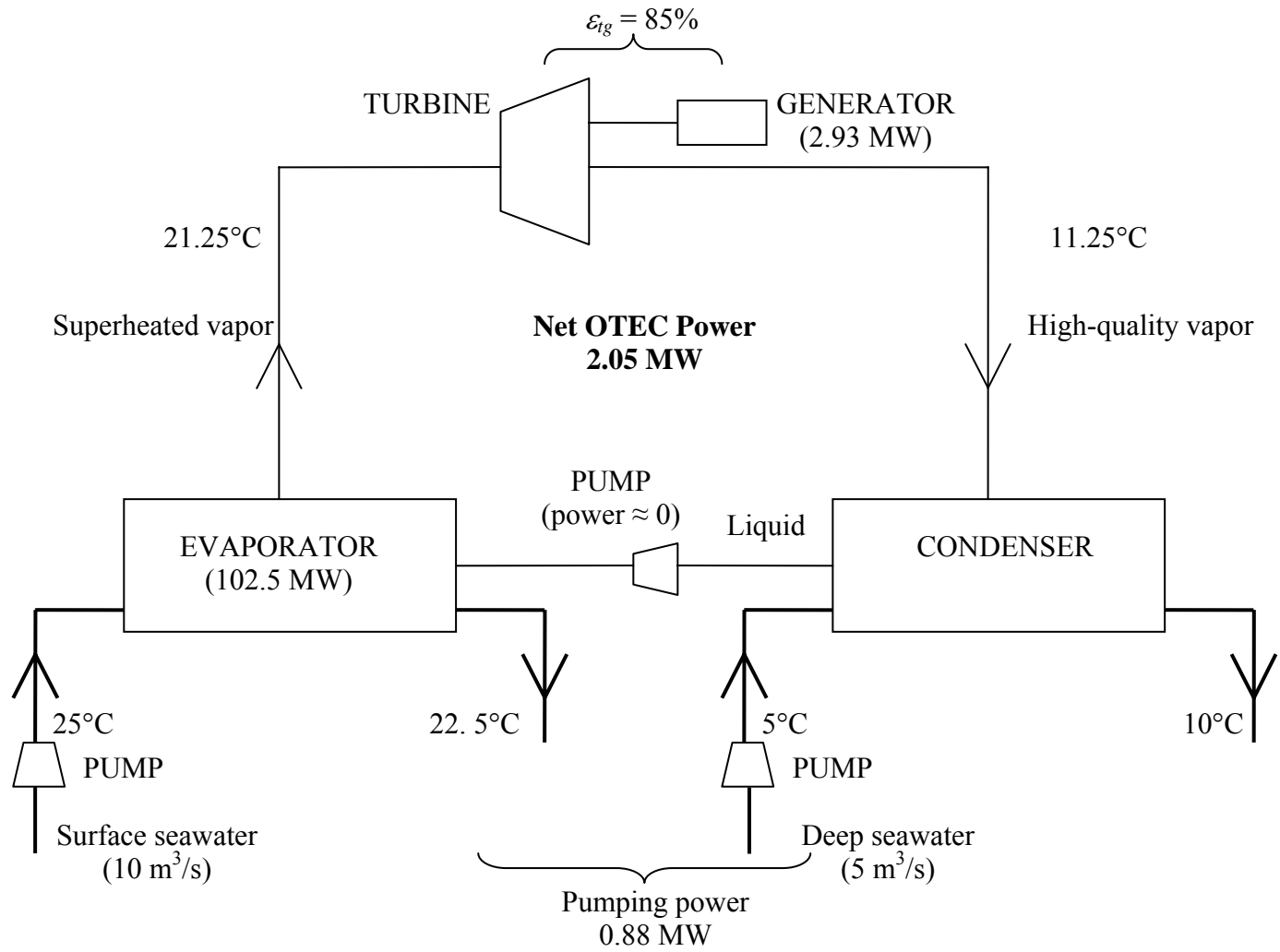


Figure 2 – Illustration of Standard OTEC Process when $\eta = 0.5$ and $Q_{ww} = 10 \text{ m}^3/\text{s}$; work ratio is 1.0 (feed pump power negligible)

Net power decreases even more sharply than P_g as ΔT drops. In fact, P_{net} would drop to zero at $\Delta T = 11^\circ\text{C}$, with $\Delta T_{design} = 20^\circ\text{C}$. It could be argued that a drop in thermal resource could be matched by an increase in flow rate, but the coefficient 0.3 (30%) representing parasitic in-plant losses, instead of being held constant, would then increase rapidly. In what follows, Eq. (2) will be used as a basis to evaluate OTEC resources. It corresponds to a total seawater flow rate intensity of $7.3 \text{ m}^3/\text{s}$ per MW (net) at design conditions (with $\eta = 0.5$.)

2.2 Oceanic Temperature Structure: Steady-State Advection-Diffusion Equations

The analysis is simplified with the adoption of a one-dimensional oceanic water column extending from the seafloor (at $z = 0$) to the bottom of a mixed layer of thickness h_m (at $z = L$.) This approach has been widely used to provide insight in otherwise fairly complex problems [16, 17]. A fundamental assumption is that the scale of OTEC operations is so large, over an area A_{OTEC} of the same order of magnitude as the total oceanic surface A , that the effect of horizontal inflow and outflow at the margins can be overlooked. Avery and Wu [5] estimated the zone corresponding to $\Delta T = 22^\circ\text{C}$ to be as large as $6 \times 10^{13} \text{ m}^2$. These authors and others [7] also show a worldwide map of the OTEC resource. As expected, it lies within subtropical latitudes. With a practical value $\Delta T_{design} = 20^\circ\text{C}$, it seems reasonable to take $A_{OTEC} \approx 10^{14} \text{ m}^2$, whereas A is about $3.7 \times 10^{14} \text{ m}^2$. A precise assessment of the possible effect of marginal horizontal flow involving waters from high latitudes on the results of this study is left for further consideration. It is believed, however, that any realistic uncertainty upper bound should be smaller than values obtained by replacing A_{OTEC} with A in what follows.

Furthermore, focus is here on steady-state solutions with a mixed-layer temperature T_0 . A stable temperature profile $\theta(z)$ can be obtained through the water column below by balancing the downward diffusion of heat with an upwelling (upward advection) of velocity w . The vertical diffusion coefficient K is taken as constant, with little loss of generality (the analysis easily could be extended, for example with a diffusion coefficient inversely proportional to $\sqrt{d\theta/dz}$.) Without extensive flow perturbations from very large scale OTEC operations, the steady-state equation for $\theta(z)$ is:

$$-K \frac{d\theta}{dz} + w\theta = wT_p \quad (3)$$

where T_p is the temperature of the polar water downwelled from the margins of this one-dimensional ocean over the entire seafloor. Eq. (3) also must satisfy the following boundary condition:

$$\theta(L) = T_0 \quad (4)$$

It follows that the unperturbed steady-state temperature profile simply is:

$$\theta(z) = T_p + \{T_0 - T_p\} \exp\left\{w \frac{z-L}{K}\right\} \quad (5)$$

If a warmer steady-state ocean is envisioned in the far future, for example as a result of an accumulation of greenhouse gases in the atmosphere, with a mixed-layer temperature $T >$

T_0 , it may not be sufficient to replace T_0 with T in Eq. (5): the upwelling rate also should be adjusted from w to w' . The strength of the polar heat sink is assumed to be constant and proportional to $w(T_0 - T_p)$ throughout the warming period; since T_p results from the formation and melting of polar ice, it also should be held constant, e.g. at 0°C . If the water being cooled before downwelling at the polar margins is provided from a mixed layer at T , it follows from a heat-and-mass balance of the polar zone that:

$$w' = \frac{T_0 - T_p}{T - T_p} w \quad (6)$$

Figure 3 shows the basic and warm-ocean steady-state, unperturbed temperature profiles adopted in this study. T_0 is taken as 25°C , to be representative of tropical regions. $w = 4$ m/yr and $K = 2300$ m²/yr were selected to yield a temperature θ_{cw} of 5°C at the targeted OTEC deep water withdrawal depth of 1000 m ($z_{cw} = 3075$ m with $L = 4000$ m and a mixed layer 75 m thick.) At constant salinity, the neutral-buoyancy injection depth for OTEC mixed effluents with $\eta = 0.5$ ($\theta_{mix} = 18.33^\circ\text{C}$) is 253 m ($z_{mix} = 3822$ m.)

The choice of vertical advection rate w is typical of one-dimensional models of the ocean [18, 19.] The vertical eddy diffusion coefficient K is about half of the value proposed in early references [19], but it is in good agreement with the findings of recent and more elaborate models [20.]

For the warm-ocean condition, an increase of 4°C , i.e. $T = 29^\circ\text{C}$ is considered; it corresponds to an approximate tripling of pre-industrial atmospheric carbon dioxide concentrations. This

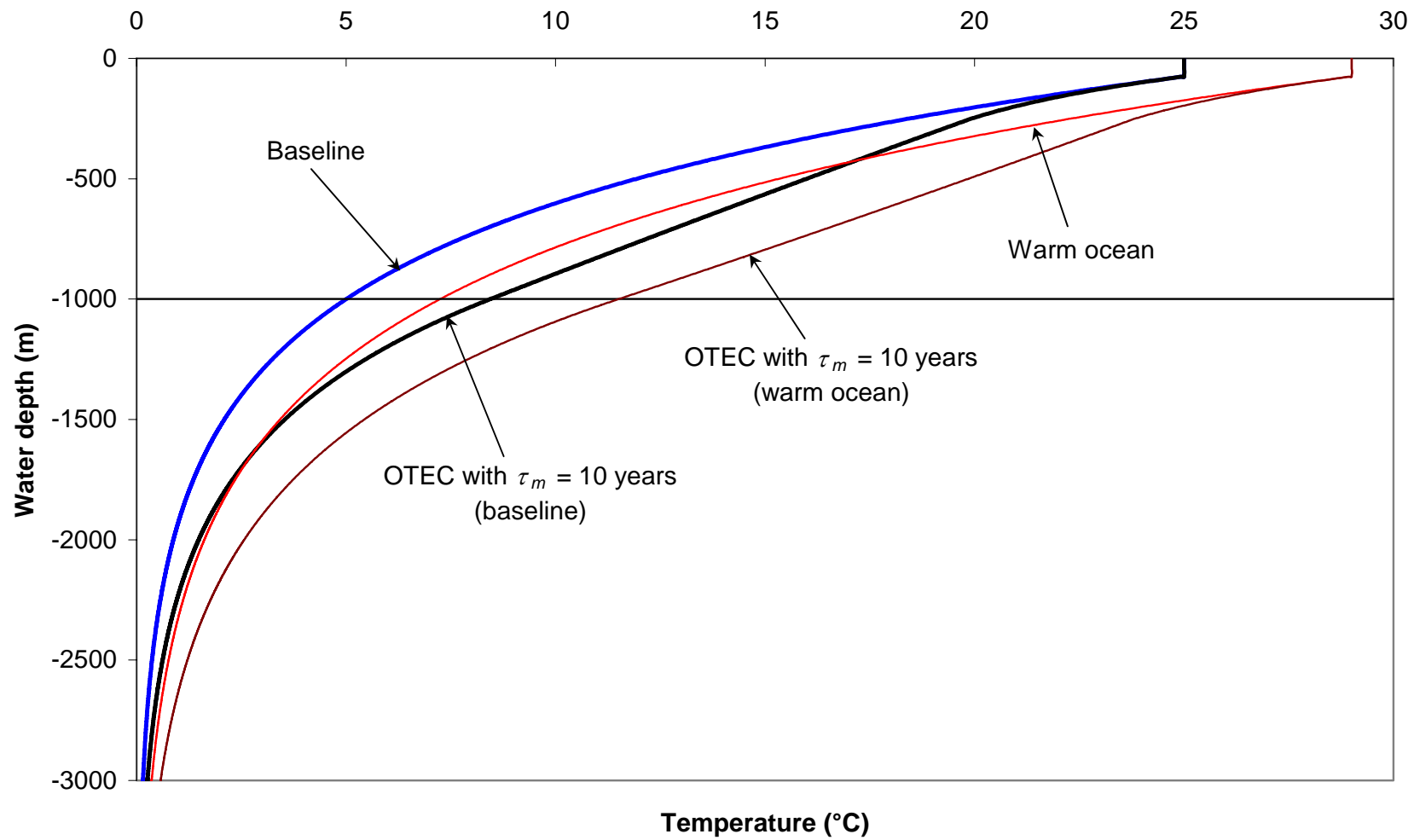


Figure 3 - Oceanic temperature profiles: baseline, warm ocean, and OTEC with $\tau_m = 10$ years.

is representative of asymptotic (post-industrial) predictions based on the combustion of estimated fossil fuel reserves [16, 17].

In what follows, the normal-ocean condition is implicit unless otherwise specified. The steady-state effect of massive OTEC operations is now examined by defining a mixed-layer utilization time τ_m , such that the combined warm-water intake flow rate from all OTEC operations would be:

$$Q_{ww} = \frac{A_{OTEC} h_m}{\tau_m} \quad (7)$$

where A_{OTEC} is the oceanic surface concerned with OTEC operations. Given the standard OTEC process described in Section 2.1, the withdrawals of warm surface seawater and of cold deep seawater represent water-column heat sinks equal to $Q_{ww}\rho c_p T_0$ in the mixed layer and to $\eta Q_{ww}\rho c_p \theta_{cw}$ and at z_{cw} , respectively. There is also a heat source at z_{mix} equal to $(1 + \eta) Q_{ww}\rho c_p \theta_{mix}$. As noted earlier, the energy extracted from ocean waters in the OTEC process is so much smaller than the enthalpies of the corresponding seawater streams that θ_{mix} can be very closely approximated by $(T_0 + \eta\theta_{cw})/(1 + \eta)$. Then, the source at z_{mix} is the sum of the two OTEC sinks. This has an important and immediate consequence: the steady-state mixed-layer temperature is not affected by OTEC operations, since the net sum of all OTEC heat sources and sinks, from the seafloor to the ocean surface, is zero. This result is consistent with the time-domain calculations of Martin and Roberts [13], for a relatively closed system such as the Gulf of Mexico, which showed a rapid recovery of the surface temperature after about a decade of massive OTEC operations.

The oceanic water column below the mixed layer is substantially affected, however. The vast flow rates sustaining OTEC operations must be balanced. If this one-dimensional model is considered to be closed, equilibrium will be achieved by having an additional upwelling h_m/τ_m for $z_{mix} > z > L$, and an additional downwelling $\eta h_m/\tau_m$ for $z_{cw} > z > z_{mix}$, as illustrated in Fig. 4. The following three coupled steady-state boundary value problems are obtained, instead of Eq. (3) and (4):

$$-K \frac{d\theta}{dz} + \left(w + \frac{h_m}{\tau_m}\right)\theta = wT_p + \frac{h_m}{\tau_m}T_0 \quad (8)$$

with Eq. (4) for $z_{mix} > z > L$;

$$-K \frac{d\theta}{dz} + \left(w - \frac{\eta h_m}{\tau_m}\right)\theta = wT_p - \frac{\eta h_m}{\tau_m}\theta_{cw} \quad (9)$$

with a temperature continuity condition at $z = z_{mix}$ for $z_{cw} > z > z_{mix}$; and Eq. (3) with a temperature continuity condition at $z = z_{cw}$ for $0 > z > z_{cw}$.

Solving Eq. (8) and (4) in the upper water-column layer $z_{mix} > z > L$ yields:

$$\theta(z) = C + \{T_0 - C\} \exp\left\{\left(w + \frac{h_m}{\tau_m}\right) \frac{z - L}{K}\right\} \quad (10)$$

where $C = (wT_p + h_m T_0 / \tau_m) / (w + h_m / \tau_m)$.

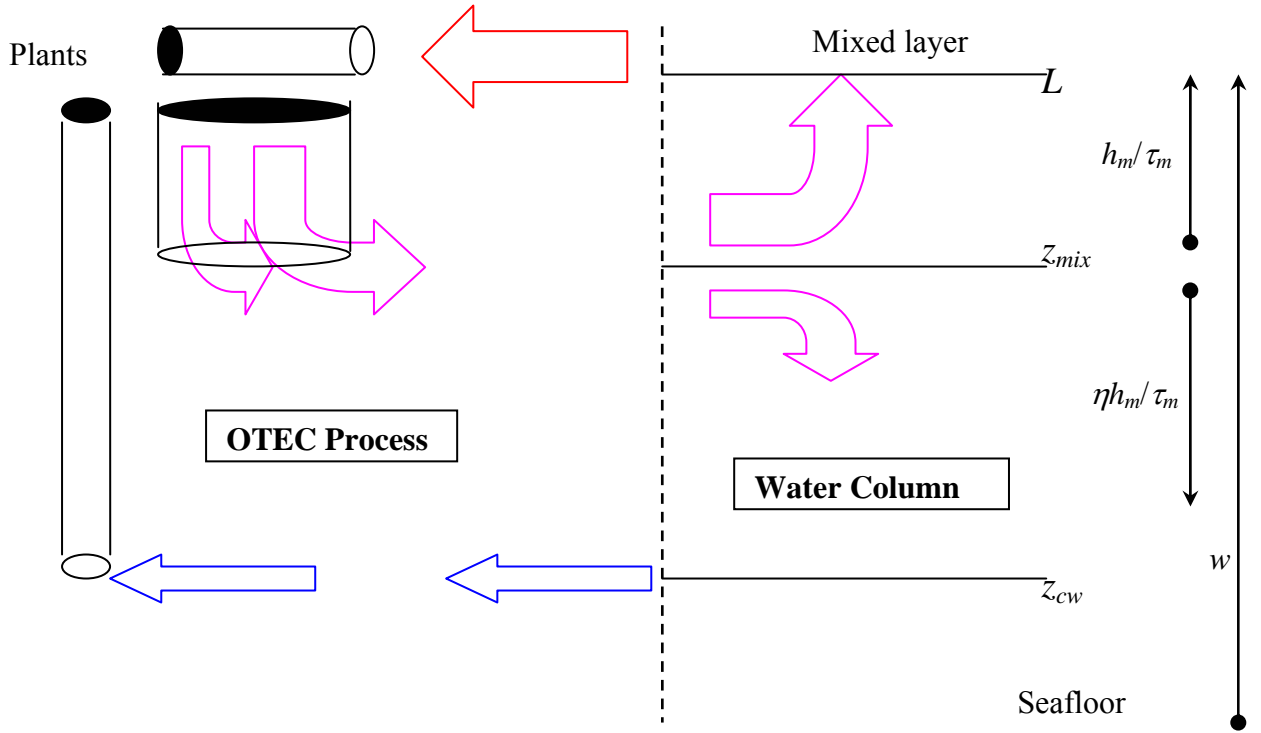


Figure 4 – Schematic of the one-dimensional model

Substituting $z = z_{mix}$ in Eq. (10) provides the continuity condition $\theta(z_{mix})$ for solving Eq. (9) in the domain $z_{cw} > z > z_{mix}$; the following temperature profile is obtained:

$$\theta(z) = D + \{\theta(z_{mix}) - D\} \exp\left\{\left(w - \frac{\eta h_m}{\tau_m}\right) \frac{z - z_{mix}}{K}\right\} \quad (11)$$

where $D = (wT_p - \eta h_m \theta_{cw} / \tau_m) / (w - \eta h_m / \tau_m)$.

Substituting $z = z_{cw}$ in Eq. (11) provides the continuity condition $\theta(z_{cw})$ as an implicit equation, for solving Eq. (3) in the domain $0 > z > z_{cw}$; the following temperature profile is obtained:

$$\theta(z) = T_p + \{\theta(z_{cw}) - T_p\} \exp(w \frac{z - z_{cw}}{K}) \quad (12)$$

Figure 3 shows the perturbed steady-state temperature profiles when $\tau_m = 10$ years, with either the baseline or warm-ocean conditions.

3.0 RESULTS AND DISCUSSION

3.1 Basic OTEC Resource Limit

The OTEC power P_{net} that can be produced in a continuous steady-state fashion (as predicted by the model described in Section 2.2.) is expected to reach a maximum as OTEC operations expand. The OTEC resource limit is understood here as this maximum P_{max} . Since the oceanic thermal structure and circulation are allowed to substantially be altered, it is highly probable that acceptable limits defined from global ecological criteria would be lower than P_{max} . Also, transient phenomena, as massive OTEC operations are developed over a significant time span, could be of considerable importance, for better or worse; this issue is left for further studies. With such caveats, P_{max} simply can be evaluated from Eq. (2) and (7), once θ_{cw} has been determined from the perturbed oceanic temperature profile. As θ_{cw} increases when τ_m decreases, P_{net} is prevented from growing linearly with flow rate, and eventually reaches a maximum: at that point, additional OTEC plants would start reducing overall OTEC power production.

Figure 5 shows P_{net} as a function of τ_m , for A_{OTEC} equal to 10^{14} m² (100 million km²). Under these circumstances, OTEC net power would peak at 2.7 TW when τ_m is 8.4 years. ΔT at maximum power would have dropped from the design value of 20°C to 15.9°C, as θ_{cw} would have warmed from 5°C to 9.1°C. In this situation, the net vertical flow already would correspond to downwelling in the layer $z_{cw} > z > z_{mix}$. The transition to net downwelling occurs when w is cancelled out by $\eta h_m / \tau_m$, i.e. when τ_m is 9.375 years. It is logical to believe that the transition to downwelling effectively would represent the case quoted by Johnson [4], whereby the OTEC deep cold seawater flow rate would match the rate at which deep water forms. Even if ΔT did not change, and even if the deep cold seawater could be drawn over A rather than A_{OTEC} , the OTEC resource corresponding to $\tau_m = 9.375$ years would be about 19 TW, i.e. much less than the range quoted in [4].

3.2 OTEC Resource Limit with a Warm Ocean

The same methodology is applied when the unperturbed steady-state ocean surface has warmed up by 4°C. As seen in Fig. 5, maximum OTEC power increases to 3.3 TW, or 20% higher, while the flow rates corresponding to the maximum essentially remain unchanged.

4.0 CONCLUSIONS

A straightforward analysis has yielded estimates of worldwide power resources that could be extracted from the steady-state operation of Ocean Thermal Energy Conversion (OTEC)

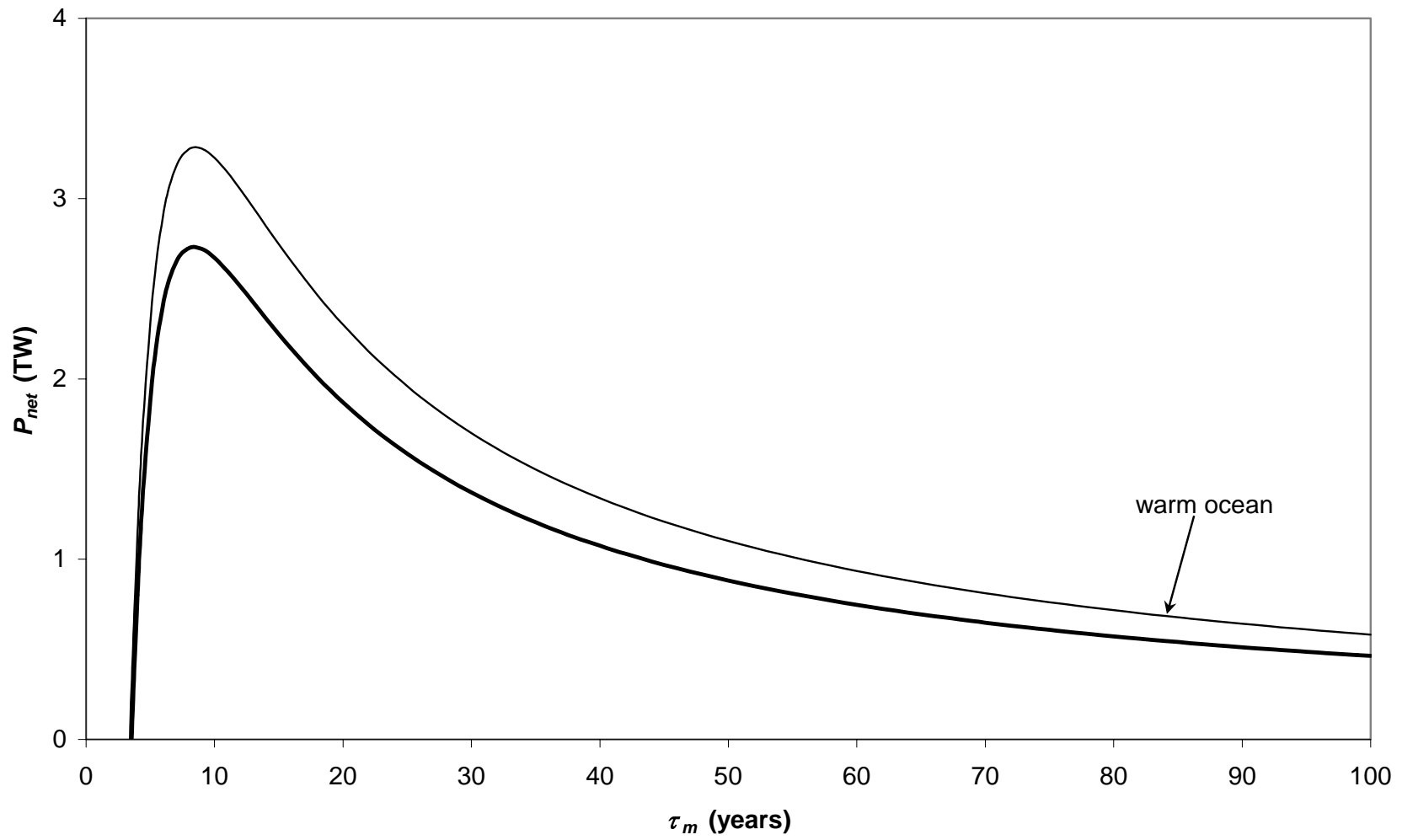


Figure 5 - Steady-state OTEC net power as a function of mixed layer utilization time

plants. While the simple one-dimensional model used here may not reproduce the complexity of a time-varying three-dimensional oceanic environment, it nevertheless captures a fundamental self-limitation of the OTEC technology: the likely disruption of the vertical thermal structure of the oceanic water column by the massive seawater flow rates needed to sustain large-scale OTEC operations. Not surprisingly, maximum OTEC power is predicted when the utilization of deep cold seawater is of the order of the average abyssal upwelling representative of the global thermohaline circulation.

According to the present study, about 3×10^9 kW (3 TW) of steady-state OTEC power may be available at most. This estimate is much smaller than values currently available in the technical literature, which are often inferred from the solar power absorbed by tropical oceans. Though perhaps disappointing to renewable energy enthusiasts, the order-of-magnitude estimate proposed here still represents a staggering amount of power. The worldwide consumption of electrical power as well as expected demands, have reached such levels that the idea of virtually unlimited OTEC energy does not hold.

Nomenclature

| | |
|-------------|---|
| A | overall oceanic surface area (m^2) |
| $A_{OTE C}$ | oceanic surface area for practical OTEC power production (m^2) |
| c_p | specific heat of seawater (J/kg-K) |
| C | auxiliary expression in Eq. (10) ($^{\circ}\text{C}$) |
| D | auxiliary expression in Eq. (11) ($^{\circ}\text{C}$) |
| h_m | mixed layer thickness (m) |
| K | vertical eddy diffusion coefficient (m^2/s) |

| | |
|-----------|---|
| L | water-column thickness below mixed layer (m) |
| P_g | OTEC gross power (W) |
| P_{max} | estimated overall OTEC net power (W) |
| P_{net} | OTEC net power (W) |
| Q_{cw} | OTEC cold deep seawater volume flow rate (m ³ /s) |
| Q_{ww} | OTEC warm surface seawater volume flow rate (m ³ /s) |
| T | surface seawater temperature in warm ocean scenario (°C) |
| T_0 | surface seawater temperature (°C) |
| T_p | polar seawater temperature (°C) |
| w | upward advection (upwelling) rate (m/s) |
| w' | upward advection (upwelling) rate in warm ocean scenario (m/s) |
| z | vertical water-column coordinate (m) |
| z_{cw} | vertical coordinate of OTEC deep seawater withdrawal (m) |
| z_{mix} | vertical coordinate of OTEC mixed effluent discharge (m) |

Greek letters

| | |
|---------------------|---|
| ΔT | temperature difference available for OTEC process (°C) |
| ΔT_{design} | design temperature difference available for OTEC process (°C) |
| ε_{tg} | turbogenerator efficiency |
| η | ratio of cold seawater flow rate over warm seawater flow rate in OTEC process |
| ρ | seawater density (kg/m ³) |
| θ | water-column temperature (°C) |

- θ_{cw} OTEC cold seawater temperature (°C)
- θ_{mix} OTEC mixed effluent temperature (°C)
- τ_m mixed layer utilization time (s)

REFERENCES

- [1] d'Arsonval, A., "Utilisation des forces naturelles. Avenir de l'électricité," *Revue Scientifique*, **17**, 370-372, 1881.
- [2] Claude, G., "Power from the Tropical Seas," *Mechanical Engineering*, **52**(12), 1039-1044, 1930.
- [3] Penney, T.R., and T.H. Daniel, "Energy from the ocean: a resource for the future," Year Book for 1989, *Encyclopædia Britannica*, 98-115, 1989.
- [4] Johnson, F.A., "Chapter 5: Closed-Cycle Ocean Thermal Energy Conversion," in Ocean Energy Recovery – The State of the Art, R. J. Seymour ed., ASCE pub., New York, 70-96, 1992.
- [5] Avery, W.H. and C. Wu, "Renewable Energy from the Ocean – A Guide to OTEC," in the Johns Hopkins University Applied Physics Laboratory Series in Science and Engineering, J.R. Apel ed., , Oxford University Press, New York, 1994.

[6] Vega, L.A., “Ocean Thermal Energy Conversion,” in Encyclopedia of Energy Technology and the Environment, Vol. 3, A. Bisio and S. Boots eds., John Wiley & Sons, New York, 2104-2119, 1995.

[7] Masutani, S.M. and P.K. Takahashi, “Ocean Thermal Energy Conversion,” in Encyclopedia of Electrical and Electronics Engineering, Vol. 15, J.G. Webster ed., John Wiley & Sons, New York, 93-103, 2000.

[8] Daniel, T.H., “Ocean Thermal Energy Conversion: An Extensive, Environmentally Benign Source of Energy for the Future,” *Sustainable Development International*, **3**, 121-125, <http://www.sustdev.org/energy/articles/energy/edition3/SDI3-10.pdf>

[9] U.S. Department of Energy, “International Energy Outlook 2004,” Report # DOE/EIA-0484(2004), available at [http://www.eia.doe.gov/oiaf/ieo/pdf/0484\(2004\).pdf](http://www.eia.doe.gov/oiaf/ieo/pdf/0484(2004).pdf) , 256 p., 2004.

[10] Zener, C., “Solar Sea Power,” *Physics Today*, **26**, 48-53, 1973.

[11] Zener, C., “The OTEC Answer to OTEC: Solar Sea Power,” *Mechanical Engineering*, **99**(12), 26-29, 1977.

[12] Penney, T.R., and D. Bharathan, “Power from the Sea,” *Scientific American*, **256**(1), 86-92, 1987.

[13] Martin, P.J., and G.O. Roberts, "An estimate of the impact of OTEC operation on the vertical distribution of heat in the Gulf of Mexico," *Proc. 4th Annual Conf. on OTEC*, 26-34, 1977.

[14] Nihous, G.C., M.A. Syed, and L.A. Vega, "Design of a Small OTEC Plant for the Production of Electricity and Fresh Water in a Pacific Island," *Proc. International Conference on Ocean Energy Recovery*, 207-216, 1989.

[15] Vega, L.A., and G.C. Nihous, "Design of a 5 MW Pre-commercial OTEC Plant", *Proc. Oceanology International '94*, **5**, 18 pp., 1994.

[16] Nihous, G.C, S.M. Masutani, L.A. Vega, and C.M. Kinoshita, "Projected Impact of Deep Ocean Carbon Dioxide Discharge on Atmospheric CO₂ Concentrations," *Climatic Change*, **27**, 225-244, 1994.

[17] Nihous, G.C, S.M. Masutani, L.A. Vega, and C.M. Kinoshita, "Preliminary Assessment of the Potential Coupling between Atmospheric Temperature and CO₂ Concentration via Ocean Water Overturning," *Energy Conversion and Management*, **37**(6-8), 1039-1048, 1996.

[18] Stommels, H. "The abyssal circulation," *Deep Sea Res.*, **5**(1), 80-82, 1958.

[19] Munk, W.H., "Abyssal recipes," *Deep Sea Res.*, **13**, 707-730, 1966.

[20] Hodnett, P.F., and R. McNamara, “A modified Stommel-Arons model of the abyssal ocean circulation,” *Math. Proc. Royal Irish Ac.*, **100A**(1), 85-104, 2000.

LIST OF TABLE AND FIGURE CAPTIONS

Table 1 - Summary of OTEC power limits from the technical literature

Figure 1 - Recent and projected World power demand

(http://www.eia.doe.gov/oiaf/ieo/excel/figure_2data.xls)

Figure 2 – Illustration of Standard OTEC Process when $\eta = 0.5$ and $Q_{ww} = 10 \text{ m}^3/\text{s}$; work ratio is 1.0 (feed pump power negligible)

Figure 3 - Oceanic temperature profiles: baseline, warm ocean, and OTEC with $t_m = 10$ years.

Figure 4 – Schematic of the one-dimensional model

Figure 5 - Steady-state OTEC net power as a function of mixed layer utilization time